Functional Significance of the Shark Na,K-ATPase N-Terminal Domain. Is the Structurally Variable N-Terminus Involved in Tissue-Specific Regulation by FXYD Proteins?†

Flemming Cornelius,*,‡,§ Yasser A. Mahmmoud,‡,§ Lara Meischke,|| and Gordon Cramb||

Department of Biophysics, University of Aarhus, Ole Worms Allé 185, DK-8000 Aarhus C, Denmark, and School of Biology, Bute Medical Buildings, University of St. Andrews, Fife KY16 9TS, United Kingdom

Received March 10, 2005; Revised Manuscript Received August 2, 2005

ABSTRACT: The proteolytic profile after mild controlled trypsin cleavage of shark rectal gland Na,K-ATPase was characterized and compared to that of pig kidney Na,K-ATPase, and conditions for achieving N-terminal cleavage of the α-subunit at the T_2 trypsin cleavage site were established. Using such conditions, the shark enzyme N-terminus was much more susceptible to proteolysis than the pig enzyme. Nevertheless, the maximum hydrolytic activity was almost unaffected for the shark enzyme, whereas it was significantly decreased for the pig kidney enzyme. The apparent ATP affinity was unchanged for shark but increased for pig enzyme after N-terminal truncation. The main common effect following N-terminal truncation of shark and pig Na,K-ATPase is a shift in the E_1-E_2 conformational equilibrium toward E_1. The phosphorylation and the main rate-limiting $E_2 \rightarrow E_1$ step are both accelerated after N-terminal truncation of the shark enzyme, but decreased significantly in the pig kidney enzyme. Some of the kinetic differences, like the acceleration of the phosphorylation reaction, following N-terminal truncation of the two preparations may be due to the fact that under the conditions used for N-terminal truncation, the C-terminal domain of the FXYD regulatory protein of the shark enzyme, PLMS or FXYD10, was also cleaved, whereas the γ or FXYD2 of the pig enzyme was not. In the shark enzyme, N-terminal truncation of the α-subunit abolished association of exogenous PLMS with the α-subunit and the functional interactions were abrogated. Moreover, PKC phosphorylation of the preparation, which relieves PLMS inhibition of Na,K-ATPase activity, exposed the N-terminal trypsin cleavage site. It is suggested that PLMS interacts functionally with the N-terminus of the shark Na,K-ATPase to control the E_1-E_2 conformational transition of the enzyme and that such interactions may be controlled by regulatory protein kinase phosphorylation of the N-terminus. Such interactions are likely in shark enzyme where PLMS has been demonstrated by cross-linking to associate with the Na,K-ATPase A-domain.

In a series of studies, Jørgensen and co-workers demonstrated that the ∼30 N-terminal amino acids of kidney Na,K-ATPase, including a lysine-rich cluster, are important for the E_1-E_2 conformational equilibrium and suggested a regulatory function of the N-terminus that could be specific to the mammalian kidney enzyme (*1*−*3*). Thus, N-terminal cleavage of these amino acids of kidney α_1 by mild trypsin treatment (at the so-called T_2 cleavage site) resulted in an enzyme with reduced hydrolytic and transport capacity (V_{max}) and altered kinetic characteristics, including a reduced K^+-phosphatase activity, a defective K^+-stimulated dephosphorylation, and a decreased sensitivity to vanadate (*4*−*6*). Blostein and co-workers recently extended this work investigating the structural basis for isoform-distinct kinetic behavior of α_1 versus α_2 isoforms using either trypsinized kidney enzyme (*7*), mutated α_1 enzyme (*8*, *9*), or $\alpha_1-\alpha_2$ chimeras (*10*, *11*). They showed that differences in the primary sequence of the N-terminus cannot themselves account for the kinetic differences between α_1 and α_2 isoforms and proposed an autoregulatory role for the A-domain that is postulated to take place by interdomain interaction of the N-terminus with the cytoplasmic TM2−TM3 and TM4−TM5 loops (*12*).

The structure of the N-terminus is variable among species and isoforms, suggesting that such autoregulation may be species-specific, but it is unknown how such interactions take place and if they are controlled. Recently, it has become clear that the Na,K-ATPase is regulated by small single-transmembrane proteins of the FXYD family (*13*−*15*). At least two of these regulatory proteins, the phospholemman (PLM or FXYD1) in the myocardium (*16*) and the phospholemman-like protein from shark (PLMS or FXYD10), contain a C-terminal multisite phosphorylation domain for protein kinases, which is likely to be important for the interaction with the Na,K-ATPase (*17*, *18*). In contrast, the kidney-specific γ-subunit (FXYD2) does not contain a multisite PKA/PKC phosphorylation domain, and γ is only phosphorylated by PKC in the presence of detergents (*19*). Thus,

† This study was supported by the Danish Medical Research Council, Aarhus University Research Foundation, the A. P. Møller Foundation, The Novo Nordic Foundation, and the Carlsberg Foundation.

* To whom correspondence should be addressed: Department of Biophysics, University of Aarhus, DK-8000 Aarhus, Denmark. Telephone: +4589422926. Fax: +4586129599. E-mail: fc@biophys.au.dk.

‡ University of Aarhus.

§ These authors contributed equally to this work.

|| University of St. Andrews.

10.1021/bi0504456 CCC: $30.25
Published on Web 09/07/2005

the $\gamma-\alpha$ interaction is apparently not controlled by protein kinase phosphorylation or dephosphorylation reactions as suggested for PLMS regulation of shark rectal Na,K-ATPase. Recently, cross-linking results have demonstrated that the interaction of the cytoplasmic part of the γ-subunit with the α-subunit of Na,K-ATPase is among loop L6−L7, loop L8−L9, and stalk segment S5 (*20*), whereas the cytoplasmic part of PLMS interacts with the shark Na,K-ATPase A-domain (*21*), which includes the N-terminus of the α-subunit. In the shark enzyme, PLMS has been shown to inhibit maximum Na,K-ATPase activity and to affect the catalytic phosphorylation reaction (*17*, *18*, *22*), whereas in the kidney Na,K-ATPase, the γ-mediated regulation affects the cytoplasmic Na^+/K^+ competition, the apparent ATP affinity, and the E_1-E_2 conformational equilibrium (*23*−*25*).

Considering that the interaction of PLMS is with the A-domain of the α-subunit and the different kinetic effects found for N-terminal truncation of kidney and shark Na,K-ATPase, we speculated if the N-terminus, which is part of the A-domain, could be involved in PLMS regulation of the shark Na,K-ATPase. Since the trypsin cleavage pattern and the kinetic effects of N-terminal truncation have not previously been investigated in preparations from shark rectal glands, and emphasizing the apparently very different modes of Na,K-ATPase regulation accomplished by γ and PLMS where the latter is modulated by protein kinases, we compared the effects of trypsin treatment of shark rectal gland and pig renal Na,K-ATPase, trying to clarify if the variable N-terminus is involved in the differential FXYD regulation in the two species. Initially, the primary sequence of shark Na,K-ATPase was determined (GenBank accession number AJ781093, manuscript in preparation) so that it could be compared with pig kidney Na,K-ATPase. Subsequently, we characterized the trypsin cleavage pattern and compared several kinetic properties of kidney and shark Na,K-ATPase before and after trypsin treatment. Finally, we investigated by cross-linking if the molecular association between PLMS and shark Na,K-ATPase was influenced by N-terminal truncation of α.

EXPERIMENTAL PROCEDURES

Na,K-ATPase Preparation and Hydrolytic Activity. In this study, purified Na,K-ATPase-containing membranes from the rectal gland of *Squalus acanthias* and from pig kidney were used. Purification of membrane fragments from shark rectal glands was as previously described (*26*). Na,K-ATPase from pig kidney outer medulla was prepared essentially as described by Jørgensen (*27*). Protein concentrations, ranging from 3 to 5 mg/mL, were determined using Peterson's modification of the Lowry method (*28*), using BSA as a standard. The specific activity of the two enzyme preparations was comparable [~30 units/mg at 37 °C and ~10.5 units/mg at 24 °C (1 unit = 1 μmol of P_i/min)]. The ATPase activity was measured either by a radioactive assay (at a subsaturating ATP concentration) in a reaction mixture containing 30 mM histidine (pH 7.4), 3 mM $MgCl_2$, 0.06% BSA, 10% glycerol, and 1−1000 μM ATP (containing 0.03 μCi of [γ-^{32}P]ATP) or, at a saturating ATP concentration (3 mM), by the method of Baginski (*29*), and variable concentrations of NaCl, KCl, and ATP as indicated in the figure legends. The turnover of the enzyme (k_{cat}, molar activity) was calculated from the protein content and the determined site number (nanomoles per milligram of protein) measured as the maximum phosphorylation level attained in 25 μM ATP, 1 mM Mg^{2+}, and 150 mM Na^+ as previously described (*30*). All kinetic measurements were performed at room temperature, 23 °C, except when otherwise stated.

Cloning and Sequencing of the Shark N-Terminus. Complementary DNA fragments of the *Squalus* Na,K-ATPase α-subunit were amplified by RT-PCR essentially as described in previous studies (*18*, *31*, *32*). In brief, the initial DNA fragments were amplified from rectal gland mRNA using degenerate, inosine-containing sense and antisense primers and the 3′ and 5′ ends of the cDNA cloned using nested gene-specific and Marathon RACE kit (Clonetech, Basingstoke, U.K.) primers. The initial degenerate primers amplified an approximate 1 kb DNA fragment between the FITC and FSBA binding sites (*33*). Specific nested 5′-RACE antisense primers were then used with the kit AP1 and AP2 primers to amplify the 5′ end of the cDNA. All amplified fragments were cloned into the pCR4-TOPO vector using Invitogen's TA cloning kit (Invitrogen, Paisley, U.K.). DNA fragments were sequenced in both directions using a Big Dye Terminator sequencing kit (Perkin-Elmer Life Sciences Biosystems, Warrington, U.K.) and sequences combined and analyzed using GenJockey II software (Biosoft, Cambridge, U.K.) (*31*, *32*).

Gel Electrophoresis and Immunoblotting. Proteins were separated using Tricine-based SDS−polyacrylamide gel electrophoresis (SDS−PAGE; 3% loading gel, 9% intermediate, and 16% resolving gels, unless indicated elsewhere). Molecular mass standards were from Bio-Rad (Hercules, CA). For immunoblotting, proteins were transferred to PVDF membranes, then washed for 1 h with PBS buffer containing 5% Tween 20, and incubated overnight at room temperature with the primary antibody. The membranes were washed again with PBS and incubated with a goat anti-rabbit antibody for 2 h. After being washed, the proteins were detected using ECL reagents (Amersham Pharmacia). For the detection of the α-subunit from shark rectal gland and pig kidney, a C-terminal-specific antibody NKA1002-1016 was used (kindly provided by J. V. Møller, Department of Biophysics, University of Aarhus). An N-terminal-specific antibody to the α-subunit of shark Na,K-ATPase was raised against the N-terminal amino acid sequence ASDKYEPAATSENA (see Figure 1). The synthetic peptide containing a C-terminal cysteine was conjugated to keyhole limpet hemocyanin and antiserum raised in rabbits. The antibody was affinity purified before use. The antigenic peptide (2.5 mg) was cross-linked to thiol-Sepharose according to the manufacturer's instructions (Amersham, Biosciences, Bucks, U.K.). After being washed, the cross-linked Sepharose beads were incubated with antiserum for 40 min at room temperature, and then poured into a column. The serum was eluted and the column washed in 50 mM Tris, 0.5 M NaCl, and 1 mM EDTA (pH 8.0). The bound antibodies were eluted with 0.1 M glycine (pH 2.5). Fractions were assessed for antibody content by SDS−PAGE (*34*) and positive fractions collected, combined, and stored at −20 °C. For detection of PLMS, an anti-PLMS antiserum was used. Anti-PLMS antiserum was prepared against purified PLMS as previously described (*18*). The antibody epitope is on the cytoplasmic face of PLMS near the membrane border and upstream from the trypsin cleavage site Lys51, since C-terminally truncated

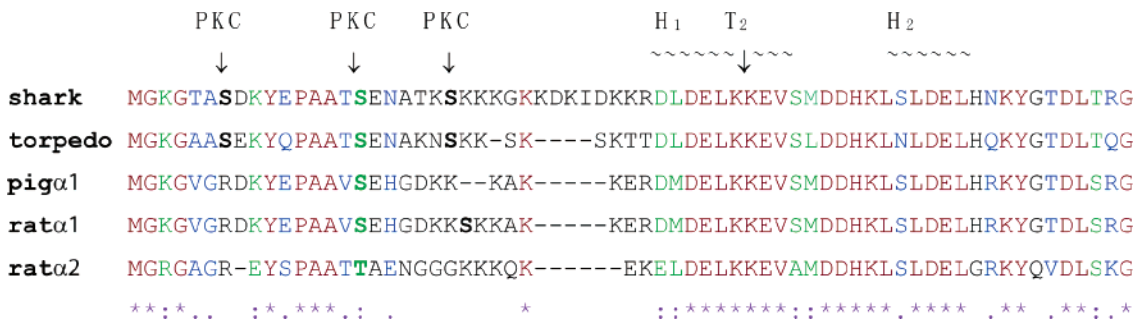

FIGURE 1: Alignment of N-terminal sequences of *S. acanthias* with that of *Torpedo californica* (GenBank accession number P05025), rat and pig α_1 (GenBank accession numbers P06685 and P05024), and rat α_2 (GenBank accession number P06686). Multiple alignment was performed using Clustal W (*55*). Conventional PKC phosphorylation sites are predicted using the Prosite database. The N-terminal trypsin cleavage site is indicated as T_2. The predicted secondary helix structures (H_1 and H_2) using Predator (*56*) and PHD (*57*) are also indicated. Note that at least in mammals the initial five amino acids are cleaved before targeting to the plasma membrane.

PLMS (at Lys51) reacts with the antibody. PLM from the myocardium also reacted with this antibody, indicating that the epitope is C^{43}RCKFNQ, since this is conserved in PLM and PLMS. The γ-subunit of the kidney enzyme was probed using anti-γ antiserum kindly provided by S. J. D. Karlish (Rehovot, Israel).

Proteolytic Cleavage of Na,K-ATPase. To obtain specific cleavage of the N-terminus of pig renal and shark rectal gland Na,K-ATPase, membrane-bound enzyme was incubated with trypsin at a trypsin to protein weight ratio of 1:20 for the shark and 1:50 for the kidney enzyme for 10−20 min on ice in the presence of 20 mM histidine (pH 7.0), 130 mM NaCl, and 1 mM EDTA. The lower trypsin concentration for the pig kidney enzyme is used to correct partially for its greater ATPase sensitivity. The reaction was stopped by addition of soy bean trypsin inhibitor at twice the amount of trypsin followed by washing. The trypsin activity was estimated using the spectroscopic measurements of the conventional esterase activity toward *p*-toluenesulfonyl-L-arginine methyl ester (TAME) (*35*). The protein content and maximum phosphoenzyme level were determined before and after N-terminal truncation to calculate the specific hydrolytic activity and molecular turnover (k_{cat}) in controls and N-terminally truncated enzyme.

To obtain specific C-terminal cleavage of PLMS at Lys51, the membrane-bound shark enzyme was incubated with trypsin at a trypsin-to-protein ratio between 1:200 and 1:1000 (w/w) for 1−10 min on ice in the presence of 20 mM histidine (pH 7.0), 1 mM EDTA, and either 130 mM NaCl or 20 mM KCl (*18*). The reaction was terminated by addition of trypsin inhibitor and the mixture diluted 10-fold with 25 mM imidazole buffer (pH 7.0) and centrifuged at 170000*g* for 1 h. After another wash, the membranes were suspended in 30 mM histidine buffer (pH 7.4) containing 25% glycerol and stored at −25 °C.

Isolation of PLMS. PLMS was isolated from shark Na,K-ATPase preparations using the extraction procedure of MacLennan (*36*). In brief, the microsomal fraction (approximately 10 mg/mL) was treated with 9 volumes of methanol and the mixture centrifuged for 10 min at 1600*g*. The supernatant was discarded, and the pellet was homogenized in 5 mL a chloroform/methanol mixture (2:1, v/v) and the mixture centrifuged again. For PLMS solubilization, the pellet from the second centrifugation was homogenized in a chloroform/methanol mixture acidified with 20 mM HCl. The mixture was centrifuged for 30 min at 48000*g*. The supernatant containing soluble PLMS in an acidic chloroform/methanol mixture was treated with 5 volumes of ethyl ether and the mixture centrifuged at 1600*g* for 10 min. Precipitated PLMS was again solubilized with an acidic chloroform/methanol mixture. The ether extraction followed by solublization was repeated at least three times. The final PLMS precipitate was suspended in an acidic chloroform/methanol mixture and kept at −20 °C. SDS−PAGE indicated a very pure preparation with a single dominating band migrating at 15 kDa that after blotting reacted with the anti-PLMS antiserum. Before addition of purified PLMS to membrane preparations, the chloroform/methanol mixture was removed on a rotary evaporator and the protein suspended in 30 mM histidine buffer (pH 7.4) containing 25% glycerol by sonication.

Cross-Linking of PLMS and α. Cross-linking with the homobifunctional thiol cross-linking agent bismaleimidohexane (BMH,[1] spacer arm length of 10.1 Å) was performed in a mixture containing 20 mM Hepes (pH 6.5), 5 mM EDTA, 50 μg of protein, and 100 μM BMH (*37*). The reaction was allowed to proceed for 30 min at 24 °C, and terminated with the addition of SDS sample buffer (*34*). Samples (4 μg) of control and cross-linked proteins were loaded onto SDS gels.

PKC Phosphorylation. Phosphorylation of shark Na,K-ATPase by PKC was performed essentially as previously described (*17*). The enzyme was incubated for 25 min at 23 °C with PKC (5 μg/mg of protein) in a reaction mixture containing 50 mM Hepes (pH 7.4), 10 mM $MgCl_2$, 0.5 mM $CaCl_2$, 10% glycerol, 0.02 mM phosphatidylserine, 0.1 μM phorbol 12-myristate 13-acetate (PMA), and 3 mM ATP (Tris salt). Following phosphorylation, control and PKC-phosphorylated enzyme were washed and homogenized in 20 mM histidine (pH 7.4) containing 25% glycerol and kept at −20 °C until use.

RH421 Fluorescence Measurements. Time-resolved RH421 fluorescence was measured using a rapid mixing stopped-flow spectrofluorimeter (SX.17MV, Applied Photophysics) as previously described (*38*). The flow volume was 100−300 μL. The excitation wavelength was 546 nm, and fluorescence was measured at emissions of ≥630 nm using a cutoff filter. The dead time for the stopped-flow apparatus was ~1.5 ms.

[1] Abbreviations: BMH, bismaleimidohexane; SEM, standard error of the mean.

Phosphorylation of the enzyme stabilized in either the E_1 or E_2 conformation was investigated by stopped-flow fluorescence measurements using the membrane probe RH421 (*38*) as previously described (*39*, *40*). In the first case, Na,K-ATPase was initially stabilized in the E_1 conformation in one syringe containing 20 μg of protein in 30 mM histidine buffer (pH 7.4) with 50 mM Na^+, 2 mM ATP, 0.1 mM EDTA, and 0.4 μg of RH421. The fluorescence increase associated with phosphorylation was followed after addition of Mg^{2+} from the second syringe containing 2.0 mL of 30 mM histidine buffer (pH 7.4) with 130 mM Na^+, 0.1 mM EDTA, and 5 mM Mg^{2+}. ATP phosphorylation of the enzyme initially stabilized in the E_2 conformation was assessed by omitting Na^+ and Mg^{2+} from syringe 1. In this case, the phosphorylation was initiated by ATP in the second syringe containing 130 mM Na^+, 0.1 mM EDTA, 5 mM Mg^{2+}, and 2 mM ATP.

Imaging and Digitizing. Scanning and intensity determination of gels were performed using ImageQuant TL image analysis software (Amersham Biosciences).

RESULTS

N-Terminal Sequence Analysis of α. In Figure 1, the N-terminal sequence of the Na,K-ATPase from the shark *S. acanthias* is shown compared to that of *Torpedo californica*, which is the closest relative with a known sequence, as well as to pig α_1 and rat α_1 and α_2.

As indicated, the Na,K-ATPase N-terminal sequences contain a highly variable lysine-rich cluster just in front of the first predicted helical segment (H_1). In shark, this sequence is extended by a four- to five-amino acid insert. This is followed by a conserved stretch containing a proteolytically sensitive lysine residue followed by the second predicted helical segment (H_2). As demonstrated by Jørgensen (*1*), the T_2 site is sensitive to trypsin cleavage when the enzyme is in the Na^+ conformation (E_1). In all five sequences, the nonconventional PKC site (Ser11, or Thr11 in rat α_2) is conserved, whereas the conventional N-terminal PKC site, Ser18 in rat, is absent in pig kidney Na,K-ATPase and replaced with glycine in the rat α_2 isoform (*41*, *42*).

Cleavage of the N-Terminus of the α*-Subunit by Trypsin.* Jørgensen (*1*−*6*) originally characterized the cleavage patterns of the kidney Na,K-ATPase α-subunit in NaCl (E_1) and KCl (E_2). In the E_1 form, mainly two cleavage sites are exposed: T_2 which is ∼30 amino acids from the N-terminal end and T_3 which is ∼250 amino acids from the N-terminal end at the TM3−A-domain interface. Following trypsin cleavage in NaCl, the Na,K-ATPase activity decreased in a biphasic manner in accordance with cleavage at these two sites. The initial fast inactivation is caused by cleavage at T_2 in which the ∼30 N-terminal amino acids are cleaved producing the so-called N-terminally truncated enzyme. This product can be difficult to resolve from the native α-subunit on SDS gels, but under optimal conditions, this trypsin split results in a band with a slightly increased mobility on SDS gels. The subsequent slower inactivation is associated with cleavage at T_3, producing a fragment with an apparent mobility on SDS gels of ∼77 kDa.

In this study, only the initial cleavage of Na,K-ATPase in the E_1 form at T_2 is investigated by employing a low trypsin:Na,K-ATPase weight ratio, short exposure time, and low temperature (0 °C). In Figure 2, the proteolytic profiles after trypsin treatment for 20 min of shark rectal gland and pig renal Na,K-ATPase are compared using a trypsin:protein weight ratio of 1:20 for the shark enzyme and 1:50 for the pig enzyme to partially compensate for the faster inhibition of the Na,K-ATPase activity of the pig enzyme than of the shark enzyme. The weight ratio was dependent on the activity of the trypsin preparation used, which was controlled by spectroscopic measurements of the conventional esterase activity toward TAME (*35*). Panels A and B of Figure 2 show immunoblots probed with C-terminal-specific and N-terminal-specific anti-α antibodies, respectively, whereas in Figure 2C, anti-PLMS or anti-γ antibodies were used as probes.

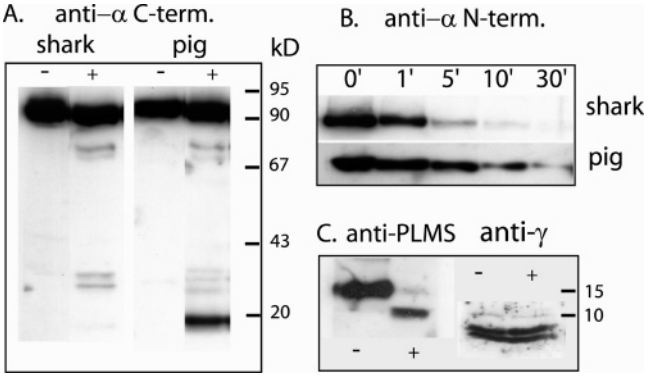

FIGURE 2: Immunoblots of shark rectal gland and pig renal Na,K-ATPase after mild trypsin treatment. Panel A shows immunoblots using shark and pig enzymes before (−) and after (+) trypsin treatment probed with a C-terminal-specific antibody to the α-subunit. In panel B, immunostaining with N-terminal-specific antibodies was used. Panel C depicts immunoblots using anti-PLMS (shark, left two lanes) or anti-γ antisera (pig, right two lanes).

As seen in Figure 2A, the proteolytic profiles of the shark rectal gland and pig renal enzymes after trypsin exposure for 20 min resemble each other qualitatively, and in both, the position of the α-subunit is shifted marginally to a smaller molecular mass indicating a slightly increased mobility following N-terminal truncation. However, the intensity of the upper band is not significantly decreased, demonstrating that cleavage outside T_2 is limited. N-Terminal truncation is, however, difficult to verify by the small shift in α mobility, but can be easily detected by immunostaining using N-terminal-specific antibodies (Figure 2B). As noted in the immunoblot using the N-terminal-specific antibody, the shark enzyme is cleaved faster at the T_2 cleavage site than the pig enzyme due to the uneven trypsin:protein conditions. This is also apparent from the imaged and digitized blots depicted in Figure 3B. In both preparations, a faint band representing a degradation product migrating at a molecular mass of ∼77 kDa, which is produced by trypsin hydrolysis at the T_3 site in the A-domain−TM3 border (*3*, *43*), is also observed, as well as a complex of low-molecular mass bands accumulated around 30−40 and ∼18 kDa representing secondary cleavage of the 77 kDa fragment (*4*). No C-terminal cleavage products migrating at ∼58 kDa representing hydrolysis at the T_1 site in the E_2 enzyme conformation (*3*, *43*) are observed. As seen from Figure 2A, the secondary cleavage patterns seem to be different in pig and shark enzyme. Time-resolved experiments (not shown) demonstrate that the secondary cleavage of the 77 kDa fragment and the 30−40 kDa fragments is appreciably faster in pig enzyme than in shark enzyme,

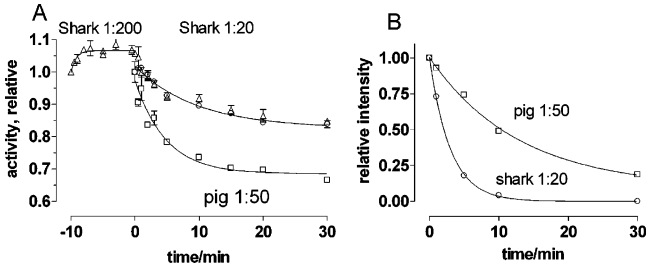

FIGURE 3: Inactivation of Na,K-ATPase activity by mild trypsin treatment. (A) Time course of hydrolytic activity as a function of trypsin treatment at 0 °C for shark (○) and pig (□) enzymes. The trypsin:protein ratio was 1:20 and 1:50 (w:w) for shark and pig enzymes, respectively. Monoexponentials with observed rate constants of 0.10 ± 0.02 (shark) and 0.21 ± 0.04 s^{-1} (pig) were fitted to the data. Also shown are results where PLMS of the shark enzyme is initially cleaved by incubation with trypsin at a trypsin:protein ratio of 1:200 followed by N-terminal truncation using the standard 1:20 trypsin:protein ratio (△). In panel B, the intensity of the immunostaining using N-terminal-specific antibodies to α is shown (cf. Figure 2B). Rate constants for the monoexponential decays were 0.08 ± 0.01 and 0.33 ± 0.01 s^{-1} for pig and shark enzymes, respectively.

resulting in a more intense 18 kDa band in the former. Moreover, the 77 kDa fragment is initially present as a single band, but later becomes resolved as a doublet, as also previously noted (*43*).

As demonstrated by the immunoblot probed with anti-PLMS antiserum, PLMS is cleaved under these mild conditions (Figure 2C, left panels). As previously shown, PLMS contains a very labile C-terminal trypsin cleavage site upstream of the multisite phosphorylation domain at Lys51 (*18*, *21*). In contrast, the pig kidney γ-subunit is resistant to the mild trypsin treatment, as indicated in the immunoblot using anti-γ antiserum by the persistence of the γ-doublets after the mild trypsin treatment (Figure 2C, right panels). It has previously been shown that the upper γ-band (γ_a) is sensitive to trypsin but only during prolonged treatment in the absence of K^+ and presence of Mg^{2+} (*44*).

In Figure 3A, the hydrolytic activity as a function of trypsin exposure at 0 °C is shown for the two enzymes using the standard trypsin:protein weight ratio of 1:20 for the shark rectal gland and 1:50 for the pig renal enzyme. The rate constants for the monoexponential inactivation are 0.10 ± 0.01 min^{-1} for the shark enzyme and 0.21 ± 0.04 min^{-1} for the pig enzyme. Thus, the pig kidney enzyme activity is significantly more labile than the shark rectal gland enzyme, even considering the higher trypsin concentration used for the shark enzyme. Using an identical trypsin:protein weight ratio, the rate constant for inactivation at 0 °C within the first 30 min is ~10 times higher for the pig renal than for the shark rectal gland enzyme. In comparing the primary sequences of the N-terminus, we find it difficult to account for such a difference (Figure 1). Indeed, the protection of the T_2 and T_3 trypsin cleavage sites in the N-terminus and A-domain of shark enzyme could be a result of a different intrinsic folding or, more likely, due to shielding either by other cytoplasmic α-domains or by the associated FXYD regulatory protein, PLMS. Actually, in all experiments the deactivation of shark Na,K-ATPase activity is preceded initially by a small activation that is correlated with the truncation of PLMS, which as previously demonstrated relieves its inhibition of the enzyme (*18*). That this small initial activation due to PLMS truncation is not the cause of the subsequent different rate of inactivation in the two preparations is demonstrated by the unchanged rate of inactivation observed if the shark enzyme is pretreated with a very small amount of trypsin to achieve selective PLMS truncation before N-terminal cleavage of the α-subunit (Figure 3A).

The decrease in hydrolytic activity seems not to be strictly correlated with the speed of removal of the N-terminus of the two enzymes, as seen by the imaged and digitized immunoblots using N-terminal-specific antibodies depicted in Figure 3B. Thus, although removal of the N-terminus is associated with inhibition in both enzyme preparations as previously demonstrated (*7*), the faster N-terminal cleavage of shark enzyme than of pig enzyme is associated with a slower inhibition rate in shark than in pig enzyme.

The steady-state levels of acid-stable phosphoenzyme (EP) of Na,K-ATPase before and after N-terminal truncation under standard conditions (1:20 and 1:50 trypsin:protein ratio for the shark and pig enzymes, respectively) were measured in the presence of 25 μM ATP, 1 mM Mg^{2+}, and 150 mM Na^+. For both shark rectal gland and pig renal enzymes, the phosphoenzyme level was unaffected by the standard trypsin treatment (typically 2.2 nmol/mg of protein for shark and 1.6 nmol/mg for pig enzyme), as previously demonstrated for kidney enzyme (*4*), indicating that the measured level of inhibition of hydrolytic activity is paralleled by a similar decrease in the rate of turnover per phosphorylation site (data not shown).

Functional Effects of N-Terminal Cleavage of the α*-Subunit.* To compare functional effects associated with N-terminal cleavage of the α-subunit of pig renal and shark rectal gland Na,K-ATPase, several steady-state properties, like alkali cation and ATP substrate dependence, or E_1-E_2 equilibrium, as well as some partial reactions such as phosphorylation reactions were studied. For the shark enzyme, a problem arises, since the mild trypsin treatment used to induce N-terminal cleavage of the α-subunit will also cleave off the C-terminal domain of PLMS (cf. Figure 2C). Therefore, the effects of N-terminal truncation of the α-subunit were compared with effects of selectively cleaving the C-terminus of PLMS (*18*, *22*). A similar problem does not exist with regard to N-terminal cleavage of the pig kidney enzyme where the γ-subunit is intact after trypsin treatment.

ATP Substrate Curve. In Figure 4, the hydrolytic activities of native and N-terminally truncated enzymes of shark and pig are shown as a function of the ATP concentration at 130 mM Na^+ and 20 mM K^+, which is optimal in the higher concentration range of ATP ([ATP] > 100 μM). Controls for the shark enzyme in which only PLMS is cleaved whereas the α-subunit is left intact are included. The C-terminal PLMS cleavage did not change the ATP activation, except for an increase in maximum hydrolytic activity, whereas N-terminal truncation of α decreased V_{max} slightly, but significantly ($p < 0.015$). As seen from Figure 4, the effects of N-terminal truncation of α on the maximum hydrolytic activity for the two enzyme preparations confirm the results given in Figure 3 that whereas V_{max} is significantly decreased for the pig kidney enzyme it is only slightly decreased in the shark enzyme. Actually, in the lower range of ATP concentrations (<100 μM), the shark Na,K-ATPase is activated both by N-terminal truncation (~15%), as also

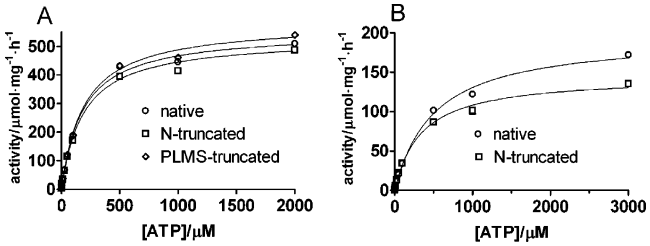

FIGURE 4: ATP substrate curves of shark (A) and pig Na,K-ATPase (B) before (○, native enzyme) and after N-terminal cleavage of α by trypsin (□). Also shown in panel A is the ATP substrate curve of the shark Na,K-ATPase preparation containing truncated PLMS (◇, PLMS-truncated). The hydrolytic activity was measured at 130 mM Na^+, 20 mM K^+, and 4 mM Mg^{2+} in 30 mM histidine buffer (pH 7.4 and 23 °C). The curves are calculated by fitting a one-site binding equation hyperbola to the data using the fitting parameters, V_{max} and K'_{ATP} (low affinity). The fitted parameters for shark enzyme are as follows: $V_{max} = 553 \pm 7$ μmol mg^{-1} h^{-1} and $K'_{ATP} = 184 \pm 8$ μM for the native enzyme, $V_{max} = 529 \pm 6$ μmol mg^{-1} h^{-1} and $K'_{ATP} = 188 \pm 8$ μM for the N-terminally truncated enzyme, and $V_{max} = 583 \pm 6$ μmol mg^{-1} h^{-1} and $K'_{ATP} = 194 \pm 8$ μM for the PLMS-truncated enzyme. The fitted parameters for pig enzyme are as follows: $V_{max} = 197 \pm 4$ μmol mg^{-1} h^{-1} and $K'_{ATP} = 508 \pm 28$ μM for the native enzyme and $V_{max} = 145 \pm 3$ μmol mg^{-1} h^{-1} and $K'_{ATP} = 341 \pm 25$ μM for the N-terminal truncated pig enzyme. The data points are means ± SEM of triplicate determinations.

previously demonstrated for the kidney enzyme (*9*), and by PLMS truncation (~40%). When the activation curve for the shark enzyme is fitted with hyperbolic curves considering only one (low-affinity) binding site, the apparent ATP affinities (K'_{ATP}) for the native and N-terminally cleaved shark rectal gland enzyme were identical (184 ± 9 and 188 ± 8 μM, respectively). For the PLMS-truncated enzyme, the K'_{ATP} was also similar, 194 ± 8 μM. For the pig kidney enzyme, the corresponding values were 508 ± 28 and 341 ± 24 μM, respectively. The two latter values were significantly different ($p < 0.001$). The decrease in K'_{ATP} for the pig kidney enzyme is almost paralleled by the decrease in V_{max} from 197 to 145 μmol mg^{-1} h^{-1}, indicating that the change in the apparent ATP-affinity is conformation-dependent rather than due to a change in the interaction of ATP with the enzyme (*45*). The values for the pig kidney enzyme confirm previous results from rat kidney, where a similar increase in the apparent ATP affinity was found after N-terminal truncation (*9*).

Na^+ and K^+ Activation of Na,K-ATPase Activity. The Na^+ activation of the shark Na,K-ATPase activity at 20 mM K^+, 3 mM Mg^{2+}, and a saturating ATP concentration (3 mM) was only slightly affected by either N-terminal truncation of α or C-terminal PLMS truncation (not shown). For both, a small but significant decrease ($p < 0.0001$) in the apparent Na^+ affinity is observed. Thus, following N-terminal truncation or PLMS truncation K'_{ATP} increases from 12.9 ± 0.1 mM in controls to 14.9 ± 0.1 mM following N-terminal truncation, and to 14.2 ± 0.2 mM following PLMS truncation.

Also, the K^+ activation of the Na-ATPase activity of the shark enzyme at saturating Na^+ (130 mM) and ATP (3 mM) concentrations was only slightly affected by N-terminal cleavage of α, or C-terminal PLMS truncation. In both cases, the apparent K^+ affinity decreased ($p < 0.0001$) with K'_K being 0.84 ± 0.13 mM for the native enzyme, 1.11 ± 0.17 mM for the N-terminally cleaved enzyme, and 1.09 ± 0.14 mM for the PLMS-truncated enzyme. The effects of PLMS truncation on apparent Na^+ and K^+ affinities are comparable to the ones previously described (*18*).

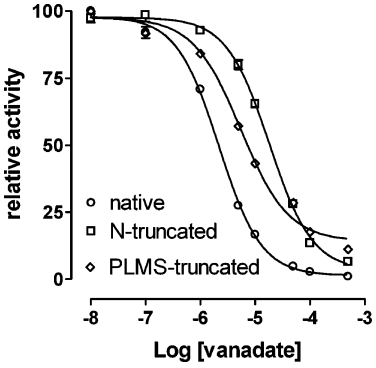

FIGURE 5: Vanadate inhibition of native, N-terminally truncated shark Na,K-ATPase, and PLMS-truncated enzymes. Hydrolytic activity is measured at 10 μM ATP, 125 mM Na^+, 5 mM K^+, and 1 mM Mg^{2+}. A sigmoid dose−response curve was fitted to the data. The inhibitor constants K_I for half-maximal inhibition of control, N-terminal truncated, and PLMS-truncated shark enzymes are 2.18 ± 0.01, 18.3 ± 0.2, and 5.51 ± 0.04 μM, respectively. The Hill coefficients were all insignificantly different from 1.0.

For the pig kidney enzyme, the same pattern of Na^+ and K^+ activation is found as for the shark enzyme (not shown) and only small changes in the cation affinities are found as a result of N-terminal truncation.

E_1−E_2 Equilibrium. Vanadate is a transition-state analogue of inorganic phosphate that binds preferentially with the E_2 conformation of the enzyme. Therefore, the enzyme sensitivity to vanadate inhibition can be used as an indication of the steady-state distribution of E_1 and E_2, as previously described (*9*). The vanadate inhibition curves for shark Na,K-ATPase before and after cleavage of the N-terminus, and after selective cleavage of PLMS, are shown in Figure 5. As seen, N-terminal truncation and PLMS truncation both right-shifted the vanadate inhibition curves, and more for the N-terminally truncated enzyme than for the PLMS-truncated enzyme. Thus, the vanadate inhibition constant, K_I, is increased ~10 times for the shark enzyme after N-terminal truncation, from ~2 μM in control to ~18 μM in the N-terminally truncated enzyme, and ~3 times to 5.5 μM in the PLMS-truncated enzyme, indicating in both cases a shift in the E_1−E_2 poise toward the E_1 conformation. Similar effects of N-terminal truncation have previously been demonstrated in mutagenesis studies using rat α_1 (*9*, *12*). We have also previously shown that PLMS truncation in itself also stabilizes the E_1 conformation as indicated by a shift in the K_I for vanadate inhibition by a factor of 3 (cf. Figure 11 in ref *18*). These changes in the steady-state E_1−E_2 equilibrium are also likely to affect other conformation-dependent steady-state properties of the enzyme like the apparent Na^+ and K^+ affinities.

Phosphorylation Reaction and E_2 to E_1 Transition. The phosphorylation reaction of the shark rectal and pig renal enzyme was investigated by stopped-flow fluorescence measurements using the membrane probe RH421 (*38*, *46*). This styryl dye partitions into the membrane containing Na,K-ATPase and is sensitive to the formation of E_2-P.

In the phosphorylation reactions, the formation of E_2-P was assessed starting the reaction from either the E_1 or E_2 conformation (*38*, *39*). Since the $E_2 \rightarrow E_1$ reaction rate-limits

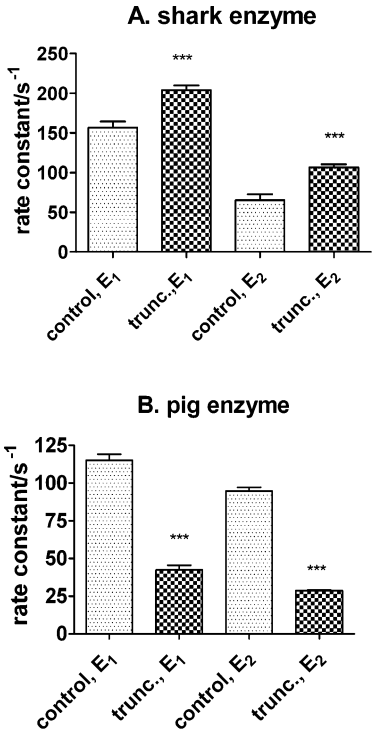

FIGURE 6: Rate constants for phosphorylation of native and N-terminally truncated shark enzyme (A) or pig kidney enzyme (B) when phosphorylation is initiated from enzyme initially stabilized in either the E_1 conformation (30 mM histidine, 50 mM Na^+, and 2 mM ATP) by addition of Mg^{2+} or the E_2 conformation (30 mM histidine alone) by addition of NaCl and MgATP. For the native shark enzyme stabilized in E_1 and E_2, the rate constants were 156 ± 8 and 58 ± 1 s^{-1}, respectively. After N-terminal truncation, the rate constants increased to 204 ± 6 and 107 ± 4 s^{-1}, respectively. For the native pig enzyme stabilized in E_1 and E_2, the rate constants were 115 ± 8 and 95 ± 5 s^{-1}, respectively. After N-terminal truncation, the rate constants decreased to 42 ± 6 and 28.7 ± 0.6 s^{-1}, respectively.

the subsequent reactions, the rate of this transition can be estimated from the rate of phosphorylation when the enzyme is stabilized in the E_2 conformation prior to phosphorylation. When the reaction is started from the E_1 conformation, the phosphorylation step is rate-limiting (*47*, *48*), except at low temperatures where the $E_1{\sim}P \rightarrow E_2$-P reaction may become partially rate-determining, at least in the shark enzyme (*46*). Stabilization of the E_1 conformation of the enzyme is achieved by incubation of the enzyme in Na^+ and ATP prior to phosphorylation, which is initiated by subsequent addition of Mg^{2+}, and thus represents the $E_1Na \rightarrow E_1NaATP \rightarrow E_1{\sim}P \rightarrow E_2$-P reactions. Stabilization of the enzyme in the E_2 conformation is achieved by incubation in histidine buffer in the absence of alkali cations or Mg^{2+}, and the fluorescence increase after subsequent simultaneous addition of Na^+ and MgATP represents the $E_2 \rightarrow E_1NaATP \rightarrow E_1{\sim}P \rightarrow E_2$-P reaction.

As seen from Figure 6A, the phosphorylation rate at 23 °C when the enzyme was initially in the E_1 conformation increases after N-terminal truncation from $\sim 156 \pm 8$ s^{-1} ($n = 5$) to 204 ± 6 s^{-1} ($n = 4$) ($p < 0.0001$). We have previously found a similar increase in the rate of the phosphorylation reaction of ~30% as a result of specific PLMS truncation (*18*). Thus, the increase in phosphorylation rate associated with cleavage of the α N-terminus is probably the result of the concomitant cleavage of the PLMS C-terminus.

When the phosphorylation reaction is assessed using enzyme initially stabilized in the E_2 conformation, the phosphorylation reaction is slower than if phosphorylation is initiated from the E_1 conformation, and also is accelerated after N-terminal truncation from a rate of 58 ± 1 s^{-1} ($n = 3$) to a rate of 107 ± 4 s^{-1} ($n = 4$) ($p < 0.0001$) (Figure 6A).

A somewhat different pattern is observed for the pig kidney enzyme (Figure 6B). Phosphorylation initiated from E_1 (rate constant of 115 ± 8 s^{-1}, $n = 4$) is also faster than that from E_2 (95 ± 5 s^{-1}, $n = 4$) as found for the shark enzyme. However, N-terminal truncation decreased significantly ($p < 0.0001$) the rate of the phosphorylation reaction both for the enzyme initially stabilized in E_1 (rate constant of 42 ± 6 s^{-1}, $n = 4$) and for the enzyme stabilized in E_2 (28.7 ± 0.6 s^{-1}, $n = 4$).

Interaction of PLMS with Na,K-ATPase Membranes. In a recent investigation using covalent cross-linking (*21*), we demonstrated interaction of PLMS with the A-domain of the α-subunit using the thiol cross-linker 1,4-bismaleimidyl-2,3-dihydroxybutane (BMDB, spacer arm length of 12 Å). The site of cross-linking was identified to be Cys254 in the A-domain of the α-subunit and the C-terminal Cys74 of PLMS (*21*). The same results were obtained with the homobifunctional thiol cross-linking agent bismaleimidohexane (BMH) with a slightly shorter spacer arm length of 10 Å. As seen from Figure 7, treatment of shark Na,K-ATPase with BMH cross-links endogenous PLMS and α as demonstrated by the appearance of a new band above the α band detected with anti-α or anti-PLMS antibodies in the immunoblot (Figure 7, lane 2of panel A and lane 2 of panel B).

As seen from panels A and B of Figure 7, cross-linking is absent after N-terminal truncation of α, or after C-terminal truncation of PLMS, as previously found (*21*). This is due to removal of the C-terminal Cys74 on PLMS by trypsin cleavage at Lys51. Thus, it is difficult to assess directly in such cross-linking experiments whether N-terminal truncation influences the interaction between endogenous PLMS and the α-subunit per se since the conditions used to obtain N-terminal truncation of α also cause C-terminal cleavage of PLMS (cf. Figure 2). Since PLMS is very hydrophobic, however, added purified (exogenous) PLMS will partition into the membrane preparations. Therefore, to investigate whether the N-terminus of α affected the PLMS−α interaction, cross-linking was performed under conditions where purified PLMS was added to either PLMS-truncated shark Na,K-ATPase preparations, where endogenous PLMS is cleaved, or after N-terminal truncation where both PLMS and the N-terminus are cleaved. Thus, the former serves as a positive control indicating whether exogenous PLMS can cross-link with α, since interaction with endogenous PLMS is prevented by C-terminal cleavage, whereas the latter experiment tests if the N-terminus of α is important for PLMS interaction. As seen from panels C and D of Figure 7, where the fraction of PLMS specifically associated with the α-subunit was probed by immunostaining with anti-α or anti-PLMS antiserum after incubation with BMH, cross-linking of exogenous PLMS to α is observed in the PLMS-truncated enzyme preparation, whereas it is absent in the N-terminally truncated preparation. Also noted (panel D) is PLMS−PLMS cross-linking under these conditions, indicat-

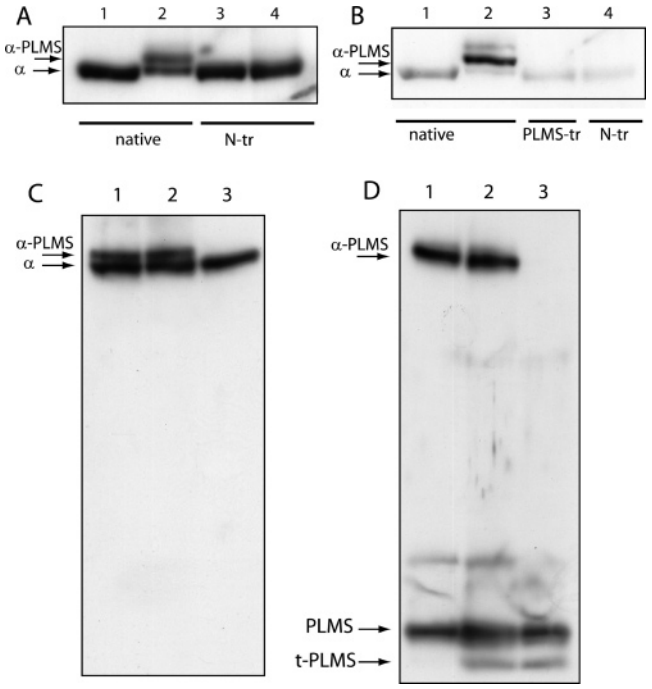

FIGURE 7: Cross-linking of endogenous and added PLMS to shark α-subunit. Cross-linking was achieved using BMH. Panels A and B show immunoblots of cross-linking of endogenous PLMS to native (lane 2), N-terminally truncated (N-tr, lane 3), or PLMS-truncated (lane 4) Na,K-ATPase compared to untreated enzyme (lane 1) as detected using either a C-terminal-specific anti-α antiserum (A) or an anti-PLMS antibody (B). As seen in lane 2 of panel A, cross-linking of PLMS and native α is indicated by the presence of a band with increased molecular mass detected by the anti-α antibody. The same band is detected in lane 2 of panel B using the anti-PLMS antibody. However, after N-terminal truncation, cross-linking products are absent as detected by immunoblotting with the anti-α antibody (panel A, lane 4) or anti-PLMS antibody (panel B, lane 4). Cross-linking of α and PLMS is also absent after truncation of endogenous PLMS (panel B, lane 3). Panels C and D show cross-linking experiments with exogenous PLMS. In panels C and D, immunoblots are shown where purified PLMS (3 μg/mg of enzyme) is added to native (lane 1), PLMS-truncated (lane 2), or N-terminally truncated (lane 3) enzymes before cross-linking and SDS−PAGE. In panel C, the anti-α antiserum is used, and in panel D, the same experiments are shown using anti-PLMS antiserum. As seen, cross-linking of exogenous PLMS is observed using PLMS-truncated enzyme preparations (lanes denoted 2) but not when PLMS is added to N-terminally truncated enzyme (lanes denoted 3). In lane 1 of panel D, endogenous PLMS is detected. In lanes 2 and 3, the 10 kDa C-terminally truncated PLMS (t-PLMS) is detected together with the added exogenous PLMS (15 kDa). The faint bands running at slightly higher molecular masses represent cross-linked PLMS−PLMS.

ing PLMS oligomerization in the membrane phase, as previously demonstrated (*17*).

Next, the effects of exogenous PLMS on Na,K-ATPase activity of native and N-terminally truncated enzymes was investigated. Thus, if purified PLMS was added to native or PLMS-truncated shark membrane preparations, the hydrolytic activity measured at 100 mM Na^+, 10 mM K^+, and 20 μM ATP was markedly changed, but not when added to the N-terminally truncated enzyme. As seen from Figure 8A, the hydrolytic activity increased and saturated when native Na,K-ATPase was used, whereas activity was inhibited in the case of the PLMS-truncated enzyme.

The amount of added PLMS giving maximum activation (0.5 μg of PLMS) corresponded to a PLMS:$\alpha\beta$ molar ratio

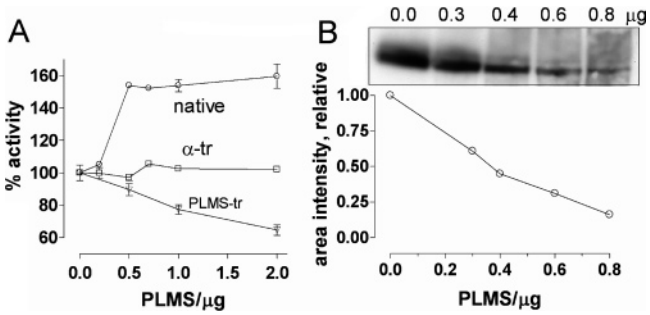

FIGURE 8: Functional interaction of shark Na,K-ATPase and exogenous PLMS. Panel A shows the effects of addition of PLMS on the Na,K-ATPase activity of native (○), PLMS-truncated (▽), or N-terminally truncated (□) shark enzyme preparations. Purified PLMS was added to the enzyme preparations (~0.5 μg) in increasing amounts up to 2 μg corresponding to a PLMS:$\alpha\beta$ molar ratio of approximately 70:1. Hydrolytic activity was measured at 20 μM ATP, 100 mM Na^+, and 10 mM K^+. The temperature was 23 °C. In panel B, an immunoblot using anti-PLMS antiserum of the cross-linked product of the native enzyme preparation and after addition of increasing amounts of PLMS is shown, as indicated in the figure, followed by cross-linking using BMH. The area intensity of the immunostaining of the cross-linked product is shown below.

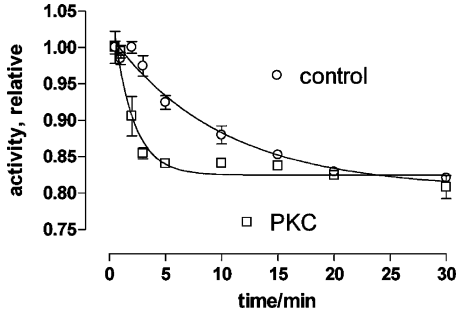

FIGURE 9: PKC phosphorylation and effects of trypsin cleavage at 0 °C on optimal Na,K-ATPase activity. The hydrolytic activity measured at 23 °C following trypsin cleavage (1:20 trypsin:protein weight ratio) was compared for shark Na,K-ATPase incubated with or without PKC in the presence of 3 mM NaCl, 15 μM EDTA, 15 μM EGTA, and 3 mM ATP. Incubation was followed by washing in imidazole buffer. After the initial activation, the hydrolytic activity decreased exponentially with rate constants of 0.10 ± 0.02 (control) and 0.58 ± 0.01 min^{-1} (PKC).

of ~17:1, assuming that all added PLMS partitions into the membranes. Paradoxically, the amount of immunostained PLMS cross-linked to native Na,K-ATPase decreased with an increasing level of addition of purified PLMS, as indicated from Figure 8B (see Discussion).

We have previously shown that PLMS can also associate with the pig renal enzyme since added purified PLMS is immunoprecipitated together with the pig kidney $\alpha\beta$-complex (*17*). However, contrary to the findings with the shark enzyme, addition of purified PLMS to the pig kidney enzyme did not affect the hydrolytic activity (not shown).

Protein Kinase Phosphorylation. To test whether the interaction of the shark N-terminus with PLMS was affected by PKC phosphorylation, we compared the sensitivity of shark Na,K-ATPase activity to trypsin treatment before and after phosphorylation by PKC. A typical result is shown in Figure 9 where the shark enzyme is preincubated with ATP in the presence or absence of PKC followed by washing and trypsin incubation. Under these conditions, PLMS is phosphorylated by PKC at the C-terminal multisite phosphorylation domain (*17*, *18*, *22*) and the α-subunit is phosphory-

lated both at the N-terminal PKC site (cf. Figure 1) and by ATP at the catalytic site. As demonstrated, the subsequent inactivation associated with N-terminal truncation of the α-subunit is appreciably faster in the PKC-treated preparation than in the control (rate constants of 0.58 ± 0.01 and 0.10 ± 0.02 min^{-1}, respectively), indicating that PKC phosphorylation exposed the N-terminal T_2 trypsin cleavage site. Since the observed accelerating effect on trypsin inactivation is only observed in the presence of PKC, phosphorylation at the catalytic site in the α-subunit is not the reason for the increased trypsin sensitivity. This is also confirmed by the identical inhibition rates for the enzyme inhibited without ATP (cf. Figure 3A) and with ATP (Figure 9).

DISCUSSION

The N-terminal segment of the kidney Na,K-ATPase α-subunit, consisting of ~30 amino acids with a sequence highly variable among species and isoforms (Figure 1), has previously been shown to affect enzyme turnover and conformational equilibrium (*1*−*12*). Different attempts have been made to pinpoint which steps in the reaction cycle are affected by various manipulations affecting the N-terminus such as truncation using trypsin cleavage, or using deletion mutants, and $\alpha_1-\alpha_2$ chimeras. The two main findings resulting from such manipulations are that N-terminal truncation of α shifts the conformational equilibrium toward E_1 and that the maximum turnover rate is decreased. Moreover, several effects of N-terminal truncation on intrinsic enzyme kinetics have emerged, like changes in the K^+ deocclusion step measured at low ATP concentrations and low temperatures (*7*−*11*), perturbed cation interaction and translocation (*49*−*51*), or changes in the transport stoichiometry (*52*). From mutagenesis studies with various deletions of N-terminal residues of the α-subunit, it was suggested that the N-terminal domain of the kidney α-subunit play an autoregulatory role in controlling the E_1-E_2 conformation of the enzyme by interaction of the N-terminus TM2−TM3 loop with the large catalytic domain (*11*).

Another line of evidence suggesting a complex function of the N-terminus is the finding in this investigation that although progressive inhibition of enzyme activity results in increasing exposure to trypsin in both the shark and pig enzymes, the rate of inactivation varies inversely with the rate of deletion of the N-terminus in the two preparations (Figure 3). The different rate of inhibition following N-terminal cleavage in shark and pig cannot be due to variable secondary cleavage at the T_3 cleavage site, which is insignificant in both preparations under the conditions described herein (cf. Figure 2). Alternatively, secondary cleavage of the N-terminally truncated enzyme outside the T_3 cleavage site leading to enhanced inhibition could be more pronounced in the pig enzyme than in the shark enzyme, although such secondary cleavage sites different from the T_3 site have not been previously described in the native kidney enzyme. From mutagenesis studies, it has been shown, however, that the hydrolytic activity is critically dependent on the number of N-terminal amino acids that are cleaved (*12*). From Figure 1, five potential trypsin cleavage sites, including T_2, can be identified in the shark N-terminal sequence. In rat kidney the split at position Lys40 leads to enhanced inhibition compared to that with the Lys32 split in kidney enzyme deletion mutants (*12*). A variable cleavage pattern in the N-terminal part of the shark and kidney preparations is difficult to invoke as an explanation for the different inhibition pattern in the two preparations since all potential trypsin splits of the shark enzyme are conserved in pig α_1.

Also, the kinetic effects resulting from N-terminal truncation of the two enzyme preparations seem to differ. Some of these effects could be related to the fact that N-terminal cleavage of the shark enzyme also leads to cleavage of PLMS, whereas in the kidney enzyme, the γ-subunit is intact after N-terminal cleavage (Figure 2C). Therefore, to separate these effects, controls incorporating data on C-terminal truncation of PLMS are included in all the kinetic investigations of the N-terminally truncated shark enzyme. Thus, whereas N-terminal truncation shifted the conformational equilibrium between the two main conformations, E_1 and E_2, toward E_1 (Figure 5) for both shark and pig kidney enzymes, the two preparations exhibited different patterns with regard to the effect of N-terminal truncation on V_{max} or the maximum rate of turnover (k_{cat}) (Figures 3 and 4): in the pig renal enzyme N-terminal truncation significantly decreased V_{max}, whereas in the shark enzyme V_{max} was only moderately decreased by 5−15%. The effect of N-terminal truncation on V_{max} and k_{cat} has previously been measured for both trypsin-treated rabbit and rat kidney enzymes (*1*−*3*, *7*) and using the recombinant N-terminally deleted enzyme (*9*). In the former, the maximum activity was only slightly decreased, when expressed per milligram of truncated enzyme, whereas in the latter, a 50% decrease in k_{cat} was found. The apparent affinity of the shark enzyme for ATP was unaffected by N-terminal truncation or C-terminal PLMS cleavage, whereas the apparent ATP affinity increased for the N-terminally truncated pig kidney enzyme (Figure 4), in accordance with results using the rat kidney enzyme (*9*). These results using the shark enzyme also confirm previous results with the kidney enzyme (*7*, *8*) that N-terminal cleavage only marginally changed the apparent affinities for Na^+ and K^+.

The $E_2 \rightarrow E_1$ reaction has been demonstrated to be the major rate-limiting step in the Na,K-ATPase reaction cycle not only at low ATP concentrations but also under physiological conditions (*39*, *53*). As seen from Figure 6, N-terminal truncation increases the rate of both the $E_2 \rightarrow E_1$ reaction and the phosphorylation reaction for the shark rectal gland enzyme at saturating ATP concentrations, whereas for the pig kidney enzyme, the rates of the $E_2 \rightarrow E_1$ reaction and the phosphorylation reaction both decrease after N-terminal truncation. Thus, the lower maximum rate of turnover of the pig kidney enzyme after N-terminal truncation could be due to a decrease in the rate of the $E_2 \rightarrow E_1$ reaction. It has previously been found that the rate of the $E_2(K_2) \rightarrow\rightarrow E_1$ reactions in kidney enzyme increases after N-terminal truncation under nonphysiological conditions of a low ATP concentration (1 μM) and a low temperature (10 °C) (*7*−*11*). The increased phosphorylation rate after N-terminal truncation of the shark enzyme is probably the result of the simultaneous PLMS cleavage, since specific cleavage of the C-terminal domain of PLMS increases the rate of phosphorylation (*14*). However, the different effect of N-terminal truncation on the $E_2 \rightarrow E_1$ reaction in shark and pig enzymes is probably not the result of the simultaneous cleavage of PLMS, which has previously been shown to increase the rate

of deocclusion of K^+ at low ATP concentrations such as in the pig kidney enzyme (*7*−*11*, *14*), but not the $E_2 \rightarrow E_1$NaATP reaction at saturating ATP concentrations (*14*). Therefore, the different kinetic effects of N-terminal truncation between shark rectal and pig renal enzymes could be due to effects from the presence of different FXYD proteins in the two preparations and their different interactions at the cytoplasmic face of the enzyme. Thus, the recently discovered difference in the spatial localization of the two associated FXYD proteins, where PLMS interacts with the A-domain near the N-terminus (*21*) and the γ-subunit interacts with α-domains further from the N-terminus near the L6−L7 and L8−L9 loops (*20*), could be important for the different kinetic effects observed in the two preparations after N-terminal truncation.

To test more directly whether the different effects of N-terminal truncation in shark and pig enzymes could be related to interactions by the FXYD proteins, the effects of N-terminal truncation on covalent cross-linking of α and PLMS were investigated (Figure 7). The results that N-terminal truncation prevented the cross-linking of exogenous PLMS with shark α, but not with the PLMS-truncated enzyme (Figure 7), demonstrate that exogenous PLMS does interact with the α-subunit and strongly indicate that the N-terminus of shark α is involved in the regulation of the interaction of α with PLMS. The absence of cross-linking of innate PLMS with both N-terminally truncated and PLMS-truncated Na,K-ATPase as detected by immunoblotting is not due to removal of the antibody-specific epitope on PLMS upon trypsin treatment, since this is retained after trypsin treatment (cf. Figure 2C); rather, the C-terminal Cys74 of PLMS (*18*) necessary for cross-linking is removed by the trypsin treatment (*21*).

Moreover, functional interactions between PLMS and the N-terminus of the α-subunit are indicated by the effects on the hydrolytic activity resulting from addition of purified PLMS to the native and PLMS-truncated shark Na,K-ATPase, but not of the N-terminally truncated enzyme (Figure 8A). The observed inhibition of the PLMS-truncated enzyme by exogenous PLMS is in accord with previous results showing that inhibition is due to interaction with the cytoplasmic domain of PLMS (*18*, *22*). The activation observed by addition of PLMS to the native enzyme could indicate that exogenous PLMS interacts differently with α than endogenous PLMS (*17*). Another explanation is suggested, however, by the cross-linking experiments using an increasing level of purified PLMS (Figure 8B), which indicate that purified PLMS competes at the transmembrane level with native Na,K-ATPase in such a way that an increasing level of exogenous PLMS decreases rather than increases the fraction of PLMS associated with Na,K-ATPase. Functional effects of exogenous transmembrane peptides caused by interaction with endogenous transmembrane domains have previously been demonstrated for a range of plasma membrane transporters, including the dopamine transporter (*54*).

As seen from Figure 9, the inactivation following N-terminal truncation by trypsin is considerably accelerated by initial PKC phosphorylation. This exposure of the T_2 trypsin cleavage site following PKC phosphorylation could be due to conformational changes induced by phosphorylation at the PKC sites located at the N-terminus (cf. Figure 1), or due to PKC-induced abrogation of the protection from trypsin attack provided by association of PLMS with the Na,K-ATPase α-subunit. Thus, the N-terminal PKC sites on the Na,K-ATPase could be involved in regulation of the PLMS−α interaction, as previously suggested (*17*, *18*, *22*).

To conclude, the data presented in this study suggest that the N-terminus of α is important for the functional interactions of PLMS with the shark α-subunit. Cross-linking experiments and kinetic investigations (*14*, *21*) both indicate that it is quite conceivable that PLMS contacts may be within the same A-domain area of the N-terminus postulated to be important for autoregulation (*12*). Such PLMS−α interaction could be controlled via protein kinase phosphorylation. Indeed, both PLMS and the N-terminus include highly charged domains and several protein kinase phosphorylation sites that could be important in regulation of electrostatic interactions. However, the possibility that PLMS may also interact and affect the α N-terminus more indirectly via its interactions with other regions of the A-domain cannot be ruled out. The conformational transitions of Na,K-ATPase involve large movements of the A-domain, and these movements probably involve complex interactions between the N-terminus and cytoplasmic TM2−TM3 loop with the catalytic TM4−TM5 loop (*12*). Thus, interaction of PLMS with the N-terminus is optimal in achieving complex regulation of Na,K-ATPase activity.

ACKNOWLEDGMENT

Hanne R. Z. Christensen, Lene Mauritzen, and Anne Lillevang are gratefully acknowledged for expert technical assistance.

REFERENCES

1. Jørgensen, P. L. (1975) Purification and characterization of (Na^+,K^+)-ATPase. V. Conformational changes in the enzyme transitions between the Na-form and the K-form studied with tryptic digestion as a tool, *Biochim. Biophys. Acta 401*, 399−415.
2. Jørgensen, P. L., Skriver, E., Hebert, H., and Maunsbach, A. B. (1982) Structure of the Na,K pump: Crystallization of pure membrane-bound Na,K-ATPase and identification of functional domains of the α-subunit, *Ann. N.Y. Acad. Sci. 402*, 207−225.
3. Jørgensen, P. L., and Collins, J. H. (1986) Tryptic and chymotryptic cleavage sites in sequence of α-subunit of (Na^++K^+)-ATPase from outer medulla of mammalian kidney, *Biochim. Biophys. Acta 860*, 570−576.
4. Jørgensen, P. L. (1977) Purification and characterization of (Na^++K^+)-ATPase. VI. Differential tryptic modification of catalytic functions of the purified enzyme in the presence of NaCl and KCl, *Biochim. Biophys. Acta 466*, 97−108.
5. Jørgensen, P. L., and Karlish, S. J. D. (1980) Defective conformational response in a selectively trypsinized (Na^++K^+)-ATPase studied with tryptophan fluorescence, *Biochim. Biophys. Acta 597*, 305−317.
6. Jørgensen, P. L., and Petersen, J. (1982) High-affinity 86Rb-binding and structural changes in the α-subunit of Na^+,K^+-ATPase as detected by tryptic digestion and fluorescence analysis, *Biochim. Biophys. Acta 705*, 38−47.
7. Wierxbicki, W., and Blostein, R. (1993) The amino-terminal segment of the catalytic subunit of kidney Na,K-ATPase regulates the potassium deocclusion pathway of the reaction cycle, *Proc. Natl. Acad. Sci. U.S.A. 90*, 70−74.
8. Daly, S. E., Lane, L. K., and Blostein, R. (1994) Functional consequences of amino-terminal diversity of the catalytic subunit of the Na,K-ATPase, *J. Biol. Chem. 269*, 23944−23948.
9. Boxenbaum, N., Daly, S. E., Javaid, Z. Z., Lane, L. K., and Blostein, R. (1998) Changes in steady-state conformational equilibrium resulting from cytoplasmic mutations of the Na,K-ATPase α-subunit, *J. Biol. Chem. 273*, 23086−23092.

10. Daly, S. E., Lane, L. K., and Blostein, R. (1996) Structure/function analysis of the amino-terminal region of the α1 and α2 subunits of Na,K-ATPase, *J. Biol. Chem. 271*, 23683−23689.
11. Segall, L., Javaid, Z. Z., Carl, S. L., Lane, L. K., and Blostein, R. (2003) Structural basis for α1 versus α2 isoform-distinct behavior of the Na,K-ATPase, *J. Biol. Chem. 278*, 9027−9034.
12. Segall, L., Lane, L. K., and Blostein, R. (2002) New insights into the role of the N terminus in conformational transitions of the Na,K-ATPase, *J. Biol. Chem. 277*, 35202−35209.
13. Crambert, G., and Geering, K. (2003) FXYD proteins: New tissue-specific regulators of the ubiquitous Na,K-ATPase, *Sci. STKE 166*, 1−9.
14. Cornelius, F., and Mahmmoud, Y. A. (2003) Functional modulation of the sodium pump: The regulatory proteins "Fixit", *News Physiol. Sci. 18*, 119−124.
15. Sweadner, K. J., and Rael, E. (2000) The FXYD gene family of small ion transport regulators or channels: cDNA sequence, protein signature sequence, and expression, *Genomics 68*, 41−56.
16. Palmer, C. J., Scott, D., and Jones, L. R. (1991) Purification and complete sequence determination of the major plasma membrane substrate for cAMP-dependent protein kinase and protein kinase C in myocardium, *J. Biol. Chem. 266*, 11126−11130.
17. Mahmmoud, Y. A., Vorum, H., and Cornelius, F. (2000) Identification of a phospholemman-like protein from shark rectal glands. Evidence for indirect regulation of Na,K-ATPase by protein kinase C via a novel member of the FXYDY family, *J. Biol. Chem. 274*, 35969−35977.
18. Mahmmoud, Y. A., Cramb, G., Maunsbach, A. B., Cutler, C. P., Meischke, L., and Cornelius, F. (2003) Regulation of Na,K-ATPase by PLMS, the phospholemman-like protein from shark: Molecular cloning, sequence, expression, cellular distribution, and functional effects of PLMS, *J. Biol. Chem. 278*, 37427−37438.
19. Mahmmoud, Y. A., and Cornelius, F. (2002) Protein kinase C phosphorylation of purified Na,K-ATPase: C-terminal phosphorylation sites at the α- and γ-subunits close to the inner face of the plasma membrane, *Biophys. J. 82*, 1909−1917.
20. Füzesi, M., Gottschalk, K.-E., Lindzen, M., Shainskaya, A., Küster, B., Garty, H., and Karlish, S. J. D. (2005) Covalent cross-links between the γ-subunit (FXYD2) and α and β subunits of Na,K-ATPase. Modeling the α−α interaction, *J. Biol. Chem. 28*, 18291−18301.
21. Mahmmoud, Y. A., Vorum, H., and Cornelius, F. (2005) Interaction of FXYD10 (PLMS) with Na,K-ATPase from shark rectal glands: Close proximity of Cys^{74} of FXYD10 to Cys^{254} in the A domain of the α-subunit revealed by intermolecular thiol cross-linking, *J. Biol. Chem. 280*, 27776−27782.
22. Cornelius, F., and Mahmmoud, Y. A. (2003) Themes in ion pump regulation, *Ann. N.Y. Acad. Sci. 986*, 579−586.
23. Therien, A. G., Karlish, S. J. D., and Blostein, R. (1999) Expression and functional role of the γ subunit of the Na,K-ATPase in mammalian cells, *J. Biol. Chem. 274*, 12252−12256.
24. Pu, H. X., Cluzeaud, F., Goldshleger, R., Karlish, S. J. D., Farman, N., and Blostein, R. (2001) Functional role and immunocytochemical localization of the γ a and γ b forms of the Na,K-ATPase γ subunit, *J. Biol. Chem. 276*, 20370−20378.
25. Arystarkhova, E., Wetzel, R. K., Asinovski, N. K., and Sweadner, K. J. (1999) The γ subunit modulates Na^+ and K^+ affinity of the renal Na,K-ATPase, *J. Biol. Chem. 274*, 33183−33185.
26. Skou, J. C., and Esmann, M. (1979) Preparation of membrane-bound and of solubilized (Na^++K^+)-ATPase from rectal glands of *Squalus acanthias*. The effect of preparative procedures on purity, specific and molar activity, *Biochim. Biophys. Acta 567*, 436−444.
27. Jørgensen, P. L. (1974) Purification and characterization of (Na^++K^+)-ATPase. 3. Purification from the outer medulla of mammalian kidney after selective removal of membrane components by sodium dodecylsulphate, *Biochim. Biophys. Acta 356*, 36−52.
28. Peterson, G. L. (1977) A simplification of the protein assay method of Lowry et al. which is more generally applicable, *Anal. Biochem. 83*, 346−356.
29. Baginski, E. S., Foa, P. P., and Zak, B. (1967) Microdetermination of inorganic phosphate, phospholipids, and total phosphate in biologic materials, *Clin. Chim. Acta 13*, 326−332.
30. Cornelius, F. (1995) Phosphorylation/dephosphorylation of reconstituted shark Na^+,K^+-ATPase: One phosphorylation site per αβ protomer, *Biochim. Biophys. Acta 1235*, 197−204.
31. Cutler, C. P., Sanders, I. L., Hazon, N., and Cramb, G. (1995) Primary sequence, tissue specificity and expression of the Na^+,K^+-ATPase α1 subunit in the European eel (*Anguilla anguilla*), *Comp. Biochem. Physiol. 111*, 567−573.
32. Cutler, C. P., Brezillon, S., Bekir, S., Sanders, I. L., Hazon, N., and Cramb, G. (2000) Expression of a duplicate Na,K-ATPase β_1-isoform in the European eel (*Anguilla anguilla*), *Am. J. Physiol. 279*, R222−R229.
33. Jørgensen, P. L. (1988) Overview: Structural basis for coupling of E1-E2 transitions in αβ-units of renal Na,K-ATPase to Na,K-translocation, *Prog. Clin. Biol. Res. 268A*, 19−38.
34. Laemmli, U. K. (1970) Cleavage of structural proteins during the assembly of the head of bacteriophage T4, *Nature 227*, 680−685.
35. Walsh, K. A. (1970) Trypsinogens and trypsins of various species, *Methods Enzymol. 19*, 41−63.
36. MacLennan, D. H. (1974) Isolation of proteins of the sarcoplasmic reticulum, *Methods Enzymol. 32*, 291−302.
37. Jones, L. R., Cornea, R. L., and Chen, Z. (2002) Close proximity between residue 30 of phospholamban and cysteine 318 of the cardiac Ca^{2+} pump revealed by intermolecular thiol cross-linking, *J. Biol. Chem. 277*, 28319−28329.
38. Fedosova, N. U., Cornelius, F., and Klodos, I. (1995) Fluorescent styryl dyes as probes for Na,K-ATPase reaction mechanism: Significance of the charge of the hydrophilic moiety of RH dyes, *Biochemistry 34*, 16806−16814.
39. Lüpfert, C., Grell, E., Pintschovius, V., Apell, H. J., Cornelius, F., and Clarke, R. J. (2001) Rate limitation of the Na^+,K^+-ATPase pump cycle, *Biophys. J. 81*, 2069−2081.
40. Cornelius, F., Turner, N., and Christensen, H. R. Z. (2003) Modulation of Na,K-ATPase by phospholipids and cholesterol. II. Steady-state and presteady-state kinetics, *Biochemistry 42*, 8541−8549.
41. Beguin, P., Beggah, A. T., Chibalin, A. V., Burgener-Kairuz, P., Jaisser, F., Mathews, P. M., Rossier, B. C., Cotecchia, S., and Geering, K. (1994) Phosphorylation of the Na,K-ATPase α-subunit by protein kinase A and C in vitro and in intact cells. Identification of a novel motif for PKC-mediated phosphorylation, *J. Biol. Chem. 269*, 24437−24445.
42. Feschenco, M. S., and Sweadner, K. J. (1995) Structural basis for species-specific differences in the phosphorylation of Na,K-ATPase by protein kinase C, *J. Biol. Chem. 270*, 14072−14077.
43. Castro, J., and Farley, R. A. (1979) Proteolytic fragmentation of the catalytic subunit of the sodium and potassium adenosine triphosphatase. Alignment of tryptic and chymotryptic fragments and location of sites labeled with ATP and iodoacetate, *J. Biol. Chem. 254*, 2221−2228.
44. Therien, A. G., Goldshleger, R., Karlish, S. J., and Blostein, R. (1997) Tissue-specific distribution and modulatory role of the γ subunit of the Na,K-ATPase, *J. Biol. Chem. 272*, 32628−32634.
45. Cleland, W. W. (1963) The kinetics of enzyme-catalyzed reactions with two or more substrates or products. III. Prediction of initial velocity and inhibition patterns by inspection, *Biochim. Biophys. Acta 67*, 188−196.
46. Cornelius, F. (1999) Rate determination in phosphorylation of shark rectal Na,K-ATPase by ATP: Temperature sensitivity and effects of ADP, *Biophys. J. 77*, 934−942.
47. Fendler, K., Jaruschewski, S., Hobbs, A., Albers, W., and Froehlich, J. P. (1993) Pre-steady-state charge translocation in Na,K-ATPase from eel electric organ, *J. Gen. Physiol. 102*, 631−666.
48. Kane, D. J., Fendler, K., Grell, E., Bamberg, E., Taniguchi, K., Froehlich, J. P., and Clarke, R. J. (1997) Stopped-flow kinetic investigations of conformational changes of pig kidney Na,K-ATPase, *Biochemistry 36*, 13406−13420.
49. Vasilets, L. A., Omay, H. S., Ohta, T., Noguchi, S., Kawamura, M., and Schwarz, W. (1991) Stimulation of the Na^+/K^+ pump by external [K^+] is regulated by voltage-dependent gating, *J. Biol. Chem. 266*, 16285−16288.
50. Vasilets, L. A., and Schwarz, W. (1993) Structure−function relationships of cation binding in the Na^+/K^+-ATPase, *Biochim. Biophys. Acta 1154*, 201−222.
51. Wang, X., Jaisser, F., and Horisberger, J.-D. (1996) Role in cation translocation of the N-terminus of the α-subunit of the Na^+−K^+ pump of Bufo, *J. Physiol. 491*, 579−594.
52. Wu, C. H., Vasilets, L. A., Takeda, K., Kawanura, M., and Schwarz, W. (2003) Functional role of the N-terminus of Na^+,K^+-ATPase α-subunit as an inactivation gate of palytoxin-induced pump channel, *Biochim. Biophys. Acta 1609*, 55−62.

53. Humphrey, P. A., Lupfert, C., Apell, H. J., Cornelius, F., and Clarke, R. J. (2002) Mechanism of the rate-determining step of the Na^+,K^+-ATPase pump cycle, *Biochemistry 41*, 9496−9507.
54. George, S. R., Ng, G. Y., Lee, S. P., Fan, T., Varghese, G., Wang, C., Deber, C. M., Seeman, P., and O'Dowd, B. F. (2003) Blockade of G protein-coupled receptors and the dopamine transporter by a transmembrane domain peptide: Novel strategy for functional inhibition of membrane proteins in vivo, *J. Pharmacol. Exp. Ther. 307*, 481−489.
55. Thompson, J. D., Higgins, D. G., and Gibson, T. J. (1994) CLUSTAL W: Improving the sensitivity of progressive multiple sequence alignment through sequence weighting, position-specific gap penalties and weight matrix choice, *Nucleic Acids Res. 22*, 4673−4680.
56. Frishman, D., and Argos, P. (1996) Incorporation of non-local interactions in protein secondary structure prediction from the amino acid sequence, *Protein Eng. 9*, 133−142.
57. Rost, B. (1996) PHD: Predicting one-dimensional protein structure by profile-based neural networks, *Methods Enzymol. 266*, 525−539.

BI0504456